

AgRP neuron hyperactivity drives hyperglycemia in a mouse model of type 2 diabetes

Yang Gou,¹ Micaela Glat,¹ Vincent Damian,¹ Caeley L. Bryan,¹ Bao Anh Phan,¹ Chelsea L. Faber,² Arikta Trivedi,¹ Matthew K. Hwang,¹ Jarrad M. Scarlett,^{1,3} Gregory J. Morton,¹ and Michael W. Schwartz¹

¹Department of Medicine, University of Washington Medicine Diabetes Institute, Seattle, Washington, USA. ²Ivy Brain Tumor Center, Department of Neurosurgery, Barrow Neurological Institute, Phoenix, Arizona, USA. ³Department of Pediatric Gastroenterology and Hepatology, Seattle Children's Hospital, Seattle, Washington, USA.

Growing evidence suggests that the pathogenesis of type 2 diabetes (T2D) involves dysfunctional central mechanisms, and, hence, the brain can be targeted to treat this disease. As an example, a single intracerebroventricular (icv) injection of fibroblast growth factor 1 (FGF1) can normalize hyperglycemia for weeks or months in rodent models of T2D. Convergent evidence implicates inhibition of a particular subset of neurons as a mediator of this FGF1 effect. Specifically, AgRP neurons, which are located in the hypothalamic arcuate nucleus (ARC) and are hyperactive in *Lep^{ob/ob}* mice and other rodent models of T2D. To investigate whether chronic AgRP neuron inactivation mimics the antidiabetic action of FGF1, we directed an adeno-associated virus (AAV) containing a cre-inducible tetanus toxin–GFP (TeTx–GFP) cassette (or cre-inducible AAV GFP control) to the ARC of obese, diabetic male *Lep^{ob/ob}* mice in which cre recombinase is expressed solely by AgRP neurons (*Lep^{ob/ob}* AgRP–Cre mice). We report that over a 10-wk period of observation, hyperglycemia was fully normalized by AgRP neuron inactivation. In contrast, changes in energy homeostasis parameters (food intake, energy expenditure, body weight, and fat mass) were not observed. We conclude that in diabetic male *Lep^{ob/ob}* mice, AgRP neuron hyperactivity is required for hyperglycemia but is dispensable for obesity.

Introduction

Work in recent decades implicates the brain both in the pathogenesis of type 2 diabetes (T2D) and as a target for its treatment (1, 2). Although based largely on preclinical evidence, the relevance of these findings to human T2D is also growing (3). Distinct afferent/sensory, integrative/processing, and efferent/motor components of this central control system continue to be identified and add to evidence of a key role for the brain in both normal and abnormal glucose homeostasis (3). Numerous preclinical studies also demonstrate that the brain can be targeted to normalize the biologically defended level of glycemia across multiple diabetic animal models (3). Yet, the specific neuronal subsets responsible for these effects remain to be identified. To address this knowledge gap, the current work investigates the role played by a specific subset of neurons — AgRP neurons located in the hypothalamic arcuate nucleus (ARC) — in the pathogenesis of T2D.

The leptin-deficient *Lep^{ob/ob}* mouse is a widely used model of T2D. In these mice, we reported in 2016 that a single intracerebroventricular (icv) injection of fibroblast growth factor 1 (FGF1) can induce diabetes remission lasting months (4). A series of subsequent studies identified AgRP neuron inhibition as a potential mediator of this sustained antidiabetic effect. For example, the anti-

diabetic effect of FGF1 was localized to the ARC and shown to require intact melanocortin 4 receptor (Mc4r) signaling (5), which is blocked by AgRP neuron activation (6). Since AgRP neurons are both hyperactive (6, 7) and inhibited in a prolonged manner following icv FGF1 injection in *Lep^{ob/ob}* mice (8), we hypothesized a key role for durable inhibition of these neurons in the sustained antidiabetic effect elicited by icv FGF1 injection.

In support of this hypothesis, we report that permanent AgRP neuron inactivation recapitulates the sustained diabetes remission induced by icv FGF1 in *Lep^{ob/ob}* mice. As this effect occurred despite having no detectable impact on food intake, energy expenditure, body weight, or body fat mass, our findings identify AgRP neurons as key drivers of hyperglycemia, but not obesity, in this T2D model.

Results

Targeting validation. To permanently inactivate AgRP neurons, a cre-inducible tetanus toxin–GFP (TeTx–GFP) AAV vector was microinjected into the ARC of *Lep^{ob/ob}* AgRP–Cre mice. Control mice received an injection of AAV containing only a cre-inducible GFP reporter (Figure 1A). Viral targeting accuracy was evaluated in both groups by detection of cre recombinase–dependent GFP fluorescence solely in the ARC (Figure 1, B and C). Three mice (out of a total of 21) were excluded on the basis of inaccurate bilateral targeting. Behavioral confirmation was provided by demonstrating a significant reduction of the refeeding response after an overnight fast among mice receiving the cre-inducible TeTx–GFP AAV compared with cre-inducible GFP controls (Figure 1D).

Effect of AgRP neuron inactivation on food intake, body weight, blood glucose, and plasma insulin levels over 10 weeks in diabetic *Lep^{ob/ob}*

Conflict of interest: The authors have declared that no conflict of interest exists.

Copyright: © 2025, Gou et al. This is an open access article published under the terms of the Creative Commons Attribution 4.0 International License.

Submitted: December 19, 2024; **Accepted:** March 12, 2025; **Published:** May 15, 2025.

Reference information: *J Clin Invest.* 2025;135(10):e189842.

<https://doi.org/10.1172/JCI189842>.

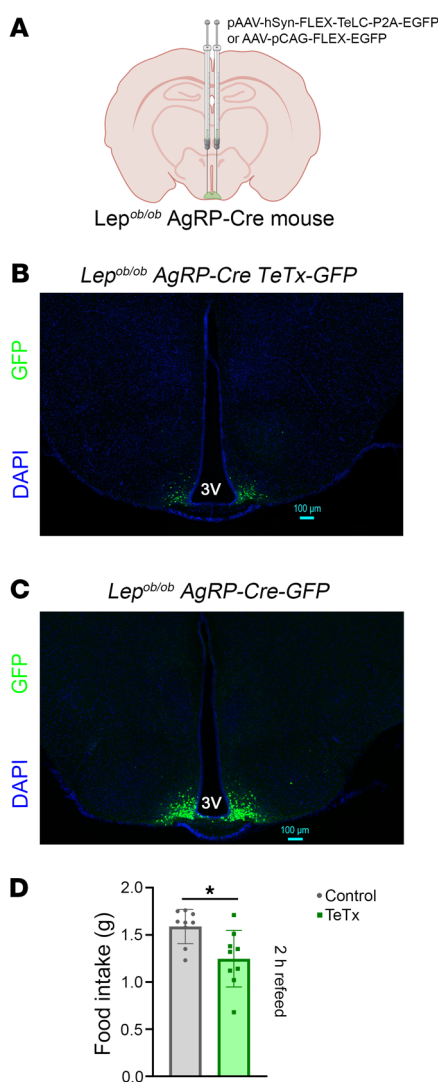


Figure 1. Validation of AgRP neuron inactivation. (A). Schematic depiction for chronic inactivation of AgRP neurons by microinjection of an AAV containing Cre-dependent GFP-fused TeTx delivered bilaterally to the arcuate nucleus (ARC) of *Lep^{ob/ob} AgRP-Cre* mice relative to a fluorescent reporter control. Stereological fluorescent images from representative animals showing (B) GFP:TeTx and (C) GFP expression in *Lep^{ob/ob} AgRP-Cre* mice. Scale bars: 100 μ m. (D) GFP:TeTx *Lep^{ob/ob} AgRP-Cre* mice ($n = 9$) exhibited a blunted refeeding response following an overnight fast when compared with those receiving the cre-inducible GFP controls ($n = 9$). 3V = third ventricle. Data are expressed as mean \pm SEM, P versus GFP control as determined by 2-tailed t-test. * $P < 0.05$.

the reduction in blood glucose levels was accompanied by a pronounced reduction in plasma insulin levels (Figure 4, A and B). Thus, increased insulin secretion is unlikely to explain the sustained remission of hyperglycemia. Similar to icv FGF1-treated mice and rats (4, 9), inactivation of AgRP neurons also had no effect on glucose tolerance, as determined by an intraperitoneal glucose tolerance test (ipGTT), as significant differences in the AUC_{glucose} curve were not detected between the 2 study groups (Figure 4, C and D).

*Potential mechanism(s) mediating the effect of AgRP neuron inactivation to normalize diabetic hyperglycemia in diabetic *Lep^{ob/ob} mice.* To investigate potential peripheral mechanisms involved in the effect of AgRP neuron inactivation to lower basal blood glucose and insulin levels, we examined liver fat and glycogen content as well as hepatic glucoregulatory gene expression (using real-time PCR). While reduced liver fat content is often associated with improvements in insulin sensitivity and glycemic control (10), no significant differences were observed between *Lep^{ob/ob} TeTx-GFP*-treated mice and their GFP controls (Figure 5A). Similarly, neither hepatic expression of the key glucoregulatory enzyme glucokinase (*Gck*) or the gluconeogenic genes phosphoenolpyruvate carboxykinase (*Pck1*) and glucose-6-phosphatase (*G6Pase*) differed between groups (Figure 5C). In contrast, liver glycogen content was significantly increased (Figure 5B), as has been observed following icv FGF1 injection in *Lep^{ob/ob} mice* (4).*

Elevated levels of plasma corticosterone and glucagon levels have each been reported in diabetic *Lep^{ob/ob} mice* (11–14) and both are implicated in diabetes pathogenesis (15, 16). We found that in *Lep^{ob/ob} mice*, plasma corticosterone levels were significantly reduced in mice with AgRP neuron inactivation relative to controls, whereas plasma glucagon levels were not significantly affected (Figure 6, A and B). Thus, suppression of hypercortisolemia (but not hyperglucagonemia) may contribute to the glucose-lowering effect elicited by inactivation of AgRP neurons. We also report that, as observed in icv FGF1-treated *Lep^{ob/ob} mice* (4, 9), plasma lactate levels were elevated in *ARC^{AgRP}-inactivated* mice relative to GFP control mice (Figure 6C), an effect that has been linked to increased hepatic glucose uptake (4, 9). Conversely, plasma free fatty acid (FFA) levels were reduced in the fed, but not the fasted, state in TeTx:GFP-treated *Lep^{ob/ob} mice* versus controls, whereas group differences in plasma triglyceride levels were not observed (Figure 6, D and E).

Discussion

The current work was undertaken to investigate neural mechanisms underlying diabetes pathogenesis: namely, the contribution made by excessive activity of hypothalamic AgRP neurons. We report

mice. The primary goal of this study was to determine the effect of AgRP neuron inactivation on serial measures of blood glucose over time in a mouse model of T2D. Among diabetic *Lep^{ob/ob} mice* in which AgRP neurons were inactivated following microinjection of a cre-inducible TeTx-GFP AAV vector into the ARC, the mean blood glucose level fell from 230 mg/dL to 140 mg/dL within the first week and was stably maintained at this level over the next 9 weeks. In contrast, the mean daily blood glucose level of diabetic *Lep^{ob/ob} GFP* controls remained well above 200 mg/dL for the entire 10-week period of observation (Figure 2A).

This outcome cannot be explained by reductions of either food intake or body weight, as neither parameter differed significantly between groups over the 10-wk course of the study (Figure 2, B and C). In addition, AgRP neuron inactivation had no effect on body composition (Figure 3, A–D), energy expenditure (Figure 3, E and F), respiratory quotient (Figure 3, G and H), or ambulatory activity (Figure 3, I and J). Thus, sustained normalization of glycemia induced by AgRP neuron inactivation in diabetic *Lep^{ob/ob} mice* is mediated independently of changes in food intake, energy expenditure, body weight, or fat mass.

Further analysis of the glucose metabolic phenotype elicited by AgRP neuron inactivation in diabetic *Lep^{ob/ob} mice* revealed that

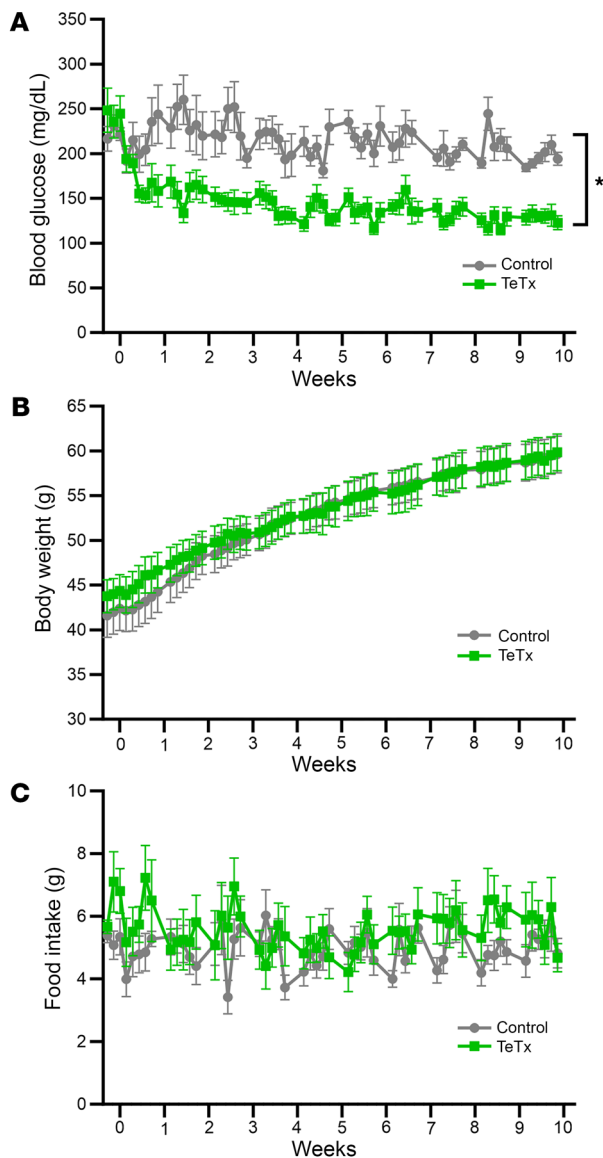


Figure 2. Permanent inactivation of AgRP neurons in *Lep^{ob/ob}* AgRP-Cre mice induces diabetes remission independent of changes in body weight and food intake. (A) Nonfasted blood glucose, (B) body weight, and (C) food intake over 10 weeks in *Lep^{ob/ob}* AgRP-Cre mice that received a bilateral injection to the arcuate nucleus (ARC) of a Cre-dependent GFP:TeTx (TeTx; $n = 9$) relative to a GFP control (Control; $n = 9$). Data are expressed as mean \pm SEM, and P versus GFP control was determined by mixed model with the Geisser-Greenhouse correction. $*P < 0.05$.

this FGF1 effect (20) and established a key role for the melanocortin system in this response. Specifically, the antidiabetic action of FGF1 is blocked by either pharmacological or genetic disruption of Mc4r signaling (5). As AgRP neuron activation also blocks Mc4r signaling, and as these neurons are hyperactive in *Lep^{ob/ob}* mice (6, 7), we identified them as potential targets for the antidiabetic action of FGF1. Consistent with this hypothesis, AgRP neurons are inhibited for at least 2 weeks following a single icv FGF1 injection (8).

In the current work we report not only that hyperglycemia is normalized comparably by icv FGF1 and AgRP neuron inactivation, but that in each case the effects are sustained for weeks or months. In addition, these effects are mediated independently of long-term changes in food intake or body fat mass; changes in serum triglyceride or plasma glucagon levels; or improvements in either glucose tolerance or hepatic steatosis. Similar to icv FGF1 injection (4, 9), inactivation of AgRP neurons is also associated with increases of both liver glycogen content and plasma lactate levels, findings suggestive of increased hepatic glucose uptake and intrahepatic glycolysis (4, 9).

Despite these similarities, some aspects of the response to AgRP neuron inactivation were not observed following icv FGF1 injection. Notable among these was the finding of reduced plasma corticosterone levels. Given that HPA axis hyperactivity is a well-documented consequence of congenital leptin deficiency in these mice (12–14), we infer from this observation that excessive AgRP neuron activity, which is also a consequence of leptin deficiency, is required for this pathological response. This interpretation is strengthened by evidence that during fasting, HPA axis activation is causally linked to AgRP neuron activation. Specifically, GABAergic neurons in the bed nucleus of the stria terminalis (BNST) that project onto and inhibit corticotropin-releasing hormone (CRH) neurons are themselves inhibited by projections from AgRP neurons lying upstream (21). Consequently, AgRP neuron activation disinhibits CRH neurons, thereby stimulating glucocorticoid secretion.

Since glucocorticoid excess (Cushing's syndrome) predisposes one to obesity and diabetes both in humans and in animal models (22), these findings support the hypothesis that reduced HPA axis activity may have contributed to sustained glucose lowering induced by AgRP neuron inactivation. This interpretation, however, raises a key question: how would a decrease of circulating glucocorticoid levels ameliorate hyperglycemia, but not obesity? While the answer is unknown, we note that, although plasma corticosterone levels were lowered by AgRP neuron inactivation, they remained higher than is typical for a WT mouse. It is therefore possible that corticosterone levels were lowered sufficiently to ameliorate hyperglycemia, but not to ameliorate hyperphagia or obesity.

Also somewhat paradoxical is the finding that, despite its clear inhibitory effect on AgRP neuron activity (8, 23), icv FGF1 injection does not lower corticosterone levels in *Lep^{ob/ob}* mice (9). Relevant to

that, in diabetic *Lep^{ob/ob}* mice, a widely used model of T2D, selective TeTx-mediated inactivation of AgRP neurons was sufficient to normalize diabetic hyperglycemia for at least 10 weeks. Since these neurons are hyperactive in *Lep^{ob/ob}* mice (6, 7) and other rodent diabetes models (17–19), we conclude that excessive AgRP neuron activity is a key driver of the diabetes phenotype of these animals. In contrast, AgRP neuron inactivation had no detectable impact on any energy homeostasis parameter (food intake, energy expenditure, respiratory quotient, body weight, or body fat mass). We conclude from these findings that AgRP neuron hyperactivity is required for the hyperglycemia of diabetic *Lep^{ob/ob}* mice but is dispensable for their hyperphagia and obesity.

Our focus on the role of the brain as a target for the treatment of T2D originated with the unexpectedly durable antidiabetic action of centrally administered FGF1. First reported in 2016 (4), a single icv FGF1 injection was shown to normalize glycemia for weeks or months across multiple rodent models of T2D (including *Lep^{ob/ob}* mice). Subsequent studies identified the ARC, which is where AgRP neurons are located, as the brain area responsible for

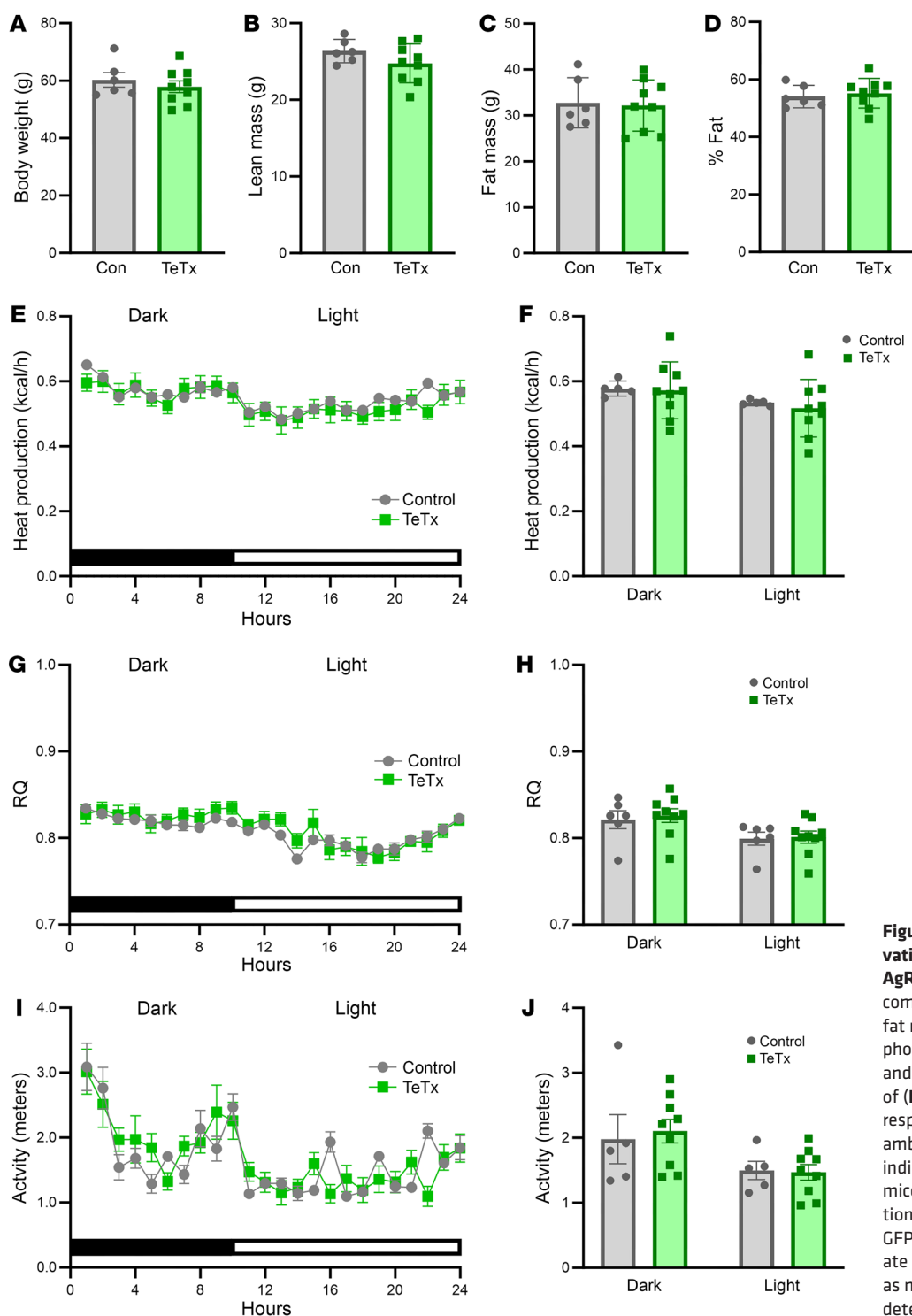


Figure 3. Effect of AgRP neuron inactivation on energy homeostasis in *Lep^{ob/ob}* AgRP-Cre mice. (A) Body weight, body composition, including (B) lean mass, (C) fat mass, and (D) percentage of fat, and photoperiod-averaged 24-hour profiles and mean dark and light cycle measures of (E and F) heat production, (G and H) respiratory quotient (RQ), and (I and J) ambulatory activity as determined using indirect calorimetry in *Lep^{ob/ob}* AgRP-Cre mice that received a bilateral microinjection of GFP:TeTx (TeTx; $n = 9$) relative to a GFP control (Control; $n = 5-9$) to the arcuate nucleus (ARC). Data are expressed as mean \pm SEM, versus GFP control as determined by 2-tailed t test.

this finding is that some AgRP neurons are not inhibited by FGF1 (8, 23). It is therefore conceivable that while the subset of AgRP neurons that drive HPA axis activity is targeted by our TeTx-based inactivation strategy, these neurons are not among those inhibited by FGF1. These considerations highlight important unanswered questions about interactions between FGF1, AgRP neurons, the HPA axis, and the pathogenesis of obesity and diabetes.

We also report that in *Lep^{ob/ob}* mice, normalization of hyperglycemia by AgRP neuron inactivation was associated with markedly

decreased plasma insulin levels. Implicit in this observation is that insulin secretion declines in response to AgRP neuron inactivation in these animals — a finding in sharp contrast to the absence of any detectable change of food intake or obesity. Thus, we infer that the pronounced hyperinsulinemia characteristic of these animals (24, 25) depends in part on AgRP neuron hyperactivity, and that this effect is not secondary to hyperphagia or obesity. Interestingly, the inhibitory effect of leptin on AgRP neurons in *Lep^{ob/ob}* mice associates with similar reductions of circulating glucose and insulin

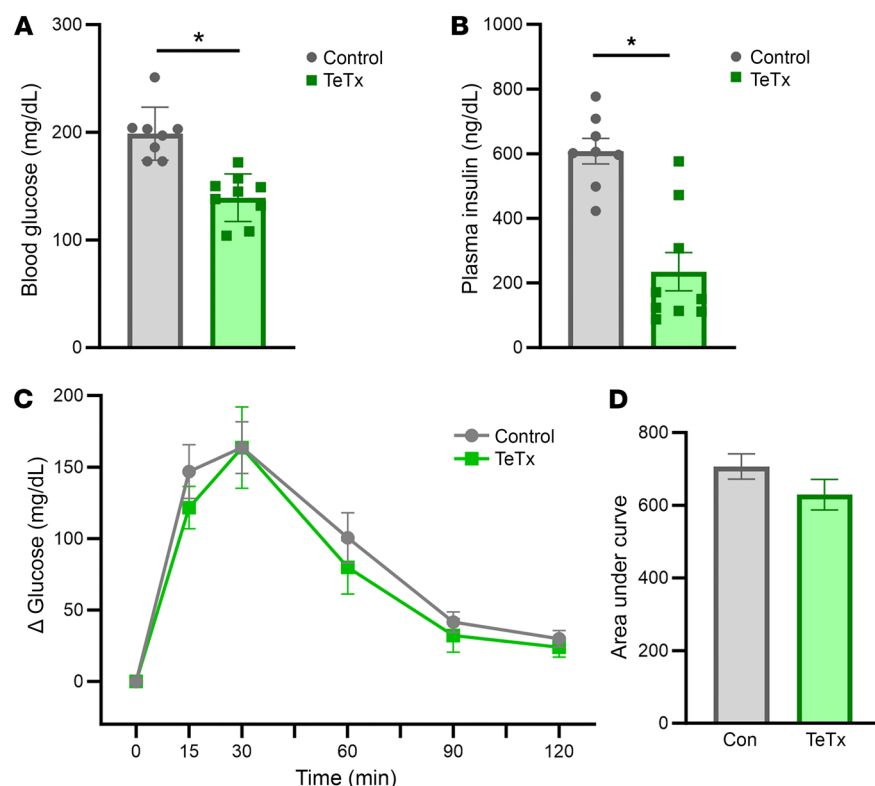


Figure 4. Effect of AgRP neuron inactivation on glucose tolerance in *Lep^{ob/ob}* AgRP-Cre mice. (A) Blood glucose and (B) plasma insulin levels, (C) changes in blood glucose levels and (D) area under the glucose curve (AUC) during an intraperitoneal glucose tolerance test (ipggt; 0.5g/kg BW) in *Lep^{ob/ob}* AgRP-Cre mice following microinjection of GFP:TeTx ($n = 9$) or GFP control ($n = 8-9$) to the arcuate nucleus (ARC). Data are expressed as mean \pm SEM, P versus GFP control as determined by 2-tailed t test. $*P < 0.05$.

stimulating POMC neurons, thereby increasing net Mc4r signaling.

Conversely, leptin-deficient states (including fasting as well as most forms of diabetes) are characterized by hyperactive AgRP neurons while POMC neurons are inhibited. By potentially inhibiting Mc4r signaling, this combination is implicated in the hyperphagia, obesity, and diabetes of leptin-deficient models, and reversal of this effect is implicated in the restoration of euglycemia to diabetic animals following central administration of either leptin (33) or FGF1 (5). Interestingly, icv leptin administration also normalizes

levels — although food intake and body weight are also reduced by leptin administration (25). Table 1 summarizes the effects of leptin, FGF1, and AgRP neuron inactivation on parameters relevant to energy and glucose homeostasis.

Located adjacent to one another in the ARC, AgRP and POMC neurons have opposing effects on Mc4r signaling in neurons lying downstream (26). Thus, whereas POMC neurons release the Mc4r agonist α -melanocyte stimulating hormone (α MSH), AgRP is an inverse agonist that inhibits Mc4r signaling (6). In addition to these opposing effects, these 2 neuronal subsets are also regulated in a reciprocal manner by diverse inputs, among them leptin and FGF1. Thus, both leptin (27–32) and FGF1 (8, 23) inhibit AgRP while

excessive glucagon secretion and HPA axis activity in uncontrolled diabetes (34), whereas icv FGF1 injection does not — and yet, both appear to inhibit AgRP neurons, activate POMC neurons, and thereby increase net melanocortin signaling.

With this background, it seems somewhat paradoxical that, unlike central leptin administration, neither icv FGF1 injection nor chronic AgRP neuron inactivation detectably impact long-term energy balance (food intake, energy expenditure, body weight, or fat mass), despite eliciting sustained normalization of hyperglycemia. Here, we consider 3 related questions raised by this paradox: (a) does AgRP neuron inhibition mediate leptin-induced anorexia; (b) does leptin act directly on AgRP neurons to inhibit them, or

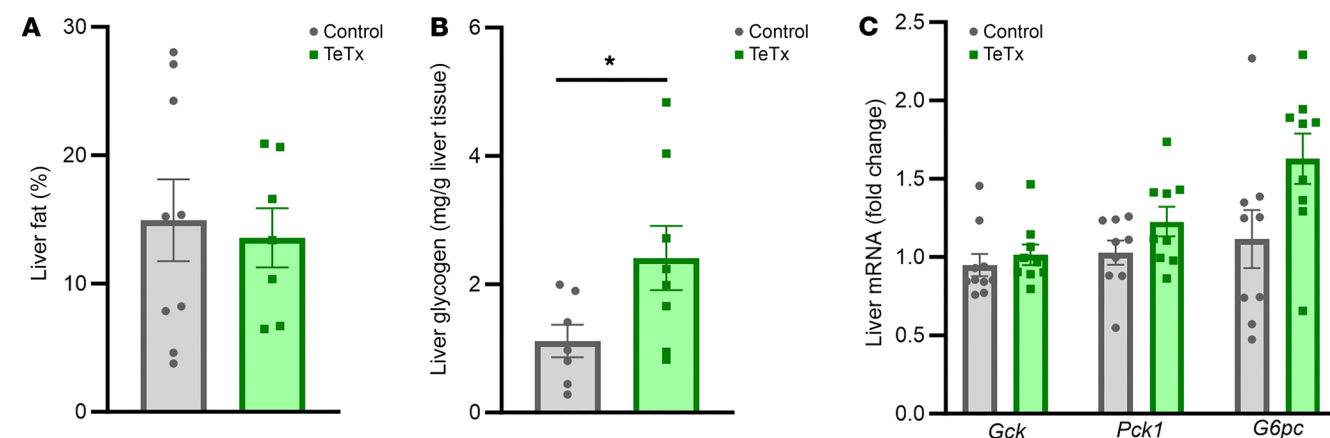


Figure 5. Effect of AgRP neuron inactivation on liver metabolism in *Lep^{ob/ob}* AgRP-Cre mice. (A) Liver fat content, (B) liver glycogen content, and (C) hepatic mRNA levels of liver glucoregulatory genes glucokinase (*Gck*), phosphoenolpyruvate carboxykinase (*Pck1*), and glucose-6-phosphatase (*G6pc*) using real-time PCR in *Lep^{ob/ob}* AgRP-Cre mice that received microinjection of GFP:TeTx ($n = 7-9$) or GFP control ($n = 7-9$) to the arcuate nucleus (ARC). Data are expressed as mean \pm SEM, P versus GFP control as determined by 2-tailed t test. $*P < 0.05$.

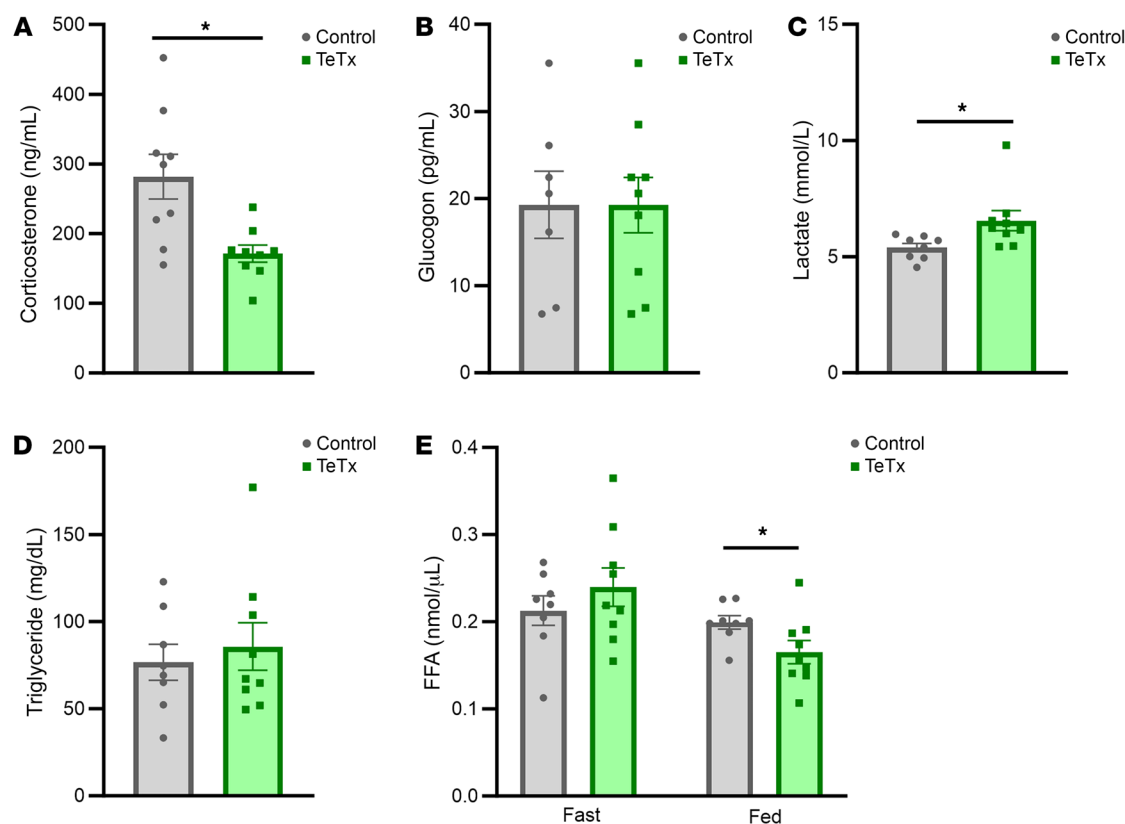


Figure 6. Inactivation of AgRP neurons lowers corticosterone levels in *Lep^{ob/ob}* AgRP-Cre mice. Plasma levels of (A) corticosterone and (B) glucagon during the mid-light cycle in the fed state. Plasma (C) lactate, (D) triglyceride (TG), and (E) free fatty acid levels in either the fed or 6-hr fasted state in *Lep^{ob/ob}* AgRP-Cre mice that received microinjection of GFP:TeTx ($n = 9$) or GFP control ($n = 7-9$) to the arcuate nucleus (ARC). Data are expressed as mean \pm SEM, P versus GFP control as determined by 2-tailed t test. * $P < 0.05$.

indirectly by activating inhibitory neurons lying upstream; and (c) are hyperphagia and obesity in leptin-deficient mice driven by activation of AgRP neurons, non-AgRP neurons, or both?

Published studies do not offer definitive answers to these questions. On the one hand, hyperphagia, obesity, and hyperglycemia were reported following acute, CRISPR-mediated leptin receptor deletion specifically from AgRP neurons in adult mice (19). This finding suggests that both energy and glucose homeostasis are constrained by direct, leptin-mediated inhibition of these neurons. A similar outcome is reported following germline deletion of leptin receptors from broad subsets of hypothalamic neurons (that include AgRP neurons, e.g., GABAergic neurons, or neurons that express the transcription factor Nkx2.1 during development (35)). Importantly, however, these effects are not recapitulated by germline deletion of leptin receptors solely from AgRP neurons (36). Together, these findings suggest that, while AgRP neuron activity in adult mice is constrained by the direct, inhibitory action of leptin, these neurons are also inhibited via actions of leptin on other neurons (e.g., activation of GABAergic neurons lying upstream (37)).

Our data extend these findings. Implied in our finding that in *Lep^{ob/ob}* mice, AgRP neuron inactivation has no detectable effect on any energy homeostasis parameter, is that leptin's potent effects on food intake and body weight in these mice must involve other neurons. Thus, we hypothesize that in these mice, hyperphagia and obesity — but not hyperglycemia — are driven by non-AgRP

neurons. While the identity of these neurons is still awaited, our findings suggest that they (a) are activated by leptin deficiency and thus are inhibited by leptin administration; (b) are sufficient to drive hyperphagia and obesity in the absence of functional AgRP neurons; and (c) are not targets for the action of FGF1. This interpretation is consistent with recent evidence that in otherwise normal mice, selective ablation of AgRP neurons has little effect on overall energy homeostasis (although it does blunt the refeeding response to a fast (38), as we observed following AgRP neuron inactivation). In addition, activation of non-AgRP, GABAergic neurons in the ARC reportedly drives severe obesity in mice (39). Identifying non-AgRP neuronal subsets that are responsible for hyperphagia and obesity — but are insufficient to drive hyperglycemia — in leptin-deficient states is a priority for future research.

Discussion of the role played by AgRP neurons in diabetes pathogenesis would be incomplete without acknowledging the 2 additional signaling molecules — neuropeptide Y (NPY) and GABA — that are expressed by and synaptically released from these neurons. Hyperactivity of AgRP neurons therefore increases signaling by NPY and GABA as well as by AgRP. Beyond being a potent orexigen (40), NPY action in the brain is reported to cause insulin resistance associated with hyperinsulinemia and reduced glucose uptake by skeletal muscle (41, 42). In addition, NPY appears to contribute to insulin resistance induced by acute stimulation of AgRP neurons, and GABA release from AgRP neu-

Table 1. Phenotypic effects of Leptin, FGF1, and AgRP neuron inactivation in *Lep^{ob/ob}* mice

Parameter	ICV FGF1	AgRP inactivation	Leptin	
Mouse model	<i>Lep^{ob/ob}</i> mice	<i>Lep^{ob/ob}</i> mice	<i>Lep^{ob/ob}</i> mice	Lean mice
Body weight	↔	↔	↓	↓
Food intake	↔	↔	↓	↓
Blood glucose	↓	↓	↓	
Plasma insulin	↔	↓	↓	↓
Glucose tolerance	↔	↔	↑	↑
Insulin tolerance	↔		↑	↑
Plasma glucagon	↔	↔	↓	
Plasma corticosterone	↔	↓	↓	
Plasma TG	↔	↔		
Plasma FFA	↔	↓	↓	↓
Liver glycogen	↑	↑	↓	↑
Liver Gck	↑	↔		
Liver Pck1	↔	↔		
Liver G6pc	↔	↔	↓	
Basal glucose uptake	↑		↑	↑
Energy expenditure		↔	↑	↔

Effects of icv FGF1 injection in *Lep^{ob/ob}* mice have been reported previously (4, 9). For a broader context, the response to leptin in both *Lep^{ob/ob}* mice and lean mice is included (25, 51–58). ↔, no change; ↓, decrease; ↑, increase.

rons has been shown to inhibit stress-activated, anorexia-inducing neurons located in the parabrachial nucleus (43). The unique contribution(s) to normal and abnormal glucose homeostasis made by synaptic release of AgRP, NPY, and GABA from AgRP neurons awaits further study.

To the extent that the effects of AgRP neuron inactivation reported herein translate to human diabetes, our finding that this intervention ameliorates hyperglycemia without apparent off-target effects identifies these neurons as potential therapeutic targets. In this context, we note that, in normal mice, AgRP neurons are rapidly inhibited following systemic administration of agonists of either GLP1 or GIP receptors (44). Given the impressive antidiabetic efficacy of this class of drugs, it will be of interest in future studies to determine whether AgRP neuron inhibition contributes to their therapeutic benefit. If so, selective, durable AgRP neuron inhibition may prove an attractive strategy for the future treatment of T2D in humans.

Methods

Sex as a biological variable

Our study exclusively examined male mice. Additional studies are required to determine whether our findings are relevant for female mice.

Animals

To permanently inactivate AgRP neurons in a mouse model of T2D, we crossed AgRP-IRES-Cre (*AgRP^{tm1(crs)Lox/J}*) mice (Jackson Laboratory, Strain no.: 012899) which were originally generated, as reported previously (45), onto *Lep^{ob/+}* (*B6.Cg-Lep^{ob}/J*) mice (Jackson Laboratory, Strain no.: 000632), to generate *Lep^{ob/ob}* AgRP-Cre mice. Only adult male, littermate mice were studied. Prior to study, all animals were individually housed in a temperature-controlled room on a 14:10 light:dark cycle under specific pathogen-free conditions with ad libitum access to

drinking water and standard laboratory chow (LabDiet), unless otherwise stated.

Stereotaxic surgeries and viral injections. AgRP neurons were permanently rendered functionally inactive in diabetic *Lep^{ob/ob}* AgRP-Cre mice by bilateral microinjection into the ARC of an AAV containing a cre-inducible TeTx-GFP cassette (*n* = 10); pAAV-hSyn-FLEX-TeLC-P2A-EYFP-WPRE (Addgene, Plasmid no. 135391 (46, 47)). Control littermate *Lep^{ob/ob}* AgRP-Cre mice received a cre-inducible AAV containing GFP only (*n* = 11) (pCAG-FLEX-EGFP-WPRE; Addgene, Plasmid no. 51502). The ARC was targeted using the following coordinates: AP: −1.4 mm; ML: ±0.3 mm; DV: −5.5 mm, and AAV was microinjected at a rate of 60 nL/min for 5 minutes (300 nL total volume), followed by a 5 minute pause and slow withdrawal. All animals received a perioperative subcutaneous injection of buprenorphine hydrochloride (0.05 mg/mL; Reckitt Benckiser). Of an initial cohort of 21 *Lep^{ob/ob}* AgRP-Cre mice, 2 mice from the AAV GFP control group and 1 from the TeTx group were excluded based

on inaccurate targeting. This resulted in a sample size of 9 in each of the 2 groups, and a targeting efficiency of 86%. Impaired AgRP neuron function was documented by reduced food intake over a 2 hour period following an overnight fast.

Criteria for sustained diabetes remission. The effect of TeTx-mediated AgRP neuron inactivation on the blood glucose level of *Lep^{ob/ob}* AgRP-Cre was compared with GFP controls over a 10 week period of observation. Consistent with previously publications (4, 9), sustained remission of diabetes was defined as continuous maintenance of blood glucose levels under 200 mg/dL. Glucose levels were measured using a hand-held glucometer (ACCU-CHEK, Roche Diabetes Care Inc.) on tail capillary blood obtained 2 hours after light cycle onset under non-fasted conditions. Daily food intake, body weight, and blood glucose levels were monitored over a period of 10 weeks.

Intraperitoneal glucose tolerance testing. Intraperitoneal glucose tolerance tests (ipGTTs) were conducted in 6 hour-fasted animals by measuring blood glucose levels at *t* = 0, 15, 30, 60, 90, and 120 minutes from a tail capillary blood sample using a hand-held glucometer (ACCU-CHEK, Roche Diabetes Care Inc.) following an i.p. injection of glucose (15% dextrose) at a dose of 0.5 g/kg body weight.

Plasma, body, and tissue composition analysis. Blood samples were collected into EDTA-treated tubes, centrifuged, and plasma removed for measurement of immunoreactive insulin, glucagon, and corticosterone by ELISA (Crystal Chem Inc.). Levels of plasma lactate (Abcam), free fatty acids (Abcam), triglycerides (RayBiotech) and liver glycogen (Abcam) were determined by enzymatic colorimetric assays. Liver glycogen content was normalized to grams wet weight after the colorimetric assay, and liver fat content was expressed as a percent of total liver mass. Total body composition and liver fat mass was measured using quantitative magnetic resonance spectroscopy (EchoMRI 3-in-1; Echo MRI) with support from the NIDDK-funded Nutrition Obesity Research Center (NORC) Energy Balance Core at the University of Washington (48).

Indirect calorimetry. For indirect calorimetry studies, *Lep^{ob/ob}* AgRP-Cre mice were acclimated to metabolic cages after which energy expenditure was measured using a computer-controlled indirect calorimetry system (Promethion; Sable Systems) with support from the NIH-funded NORC Energy Balance Core, as previously described (46, 47, 49). For each animal, O₂ consumption and CO₂ production were measured at 5 minute intervals and respiratory quotient was calculated as the ratio of CO₂ production to O₂ consumption. Energy expenditure was calculated using the Weir equation based on the rate of O₂ consumption (VO₂) (50). Ambulatory activity was measured continuously, with consecutive adjacent infrared beam breaks in the x-, y-, and z- axes scored as an activity count that was recorded every 5 minutes. Data acquisition and instrument control were coordinated by MetaScreen v.1.6.2 and raw data was processed using ExpeData v.1.4.3 (Sable Systems) using an analysis script documenting all aspects of data transformation.

IHC detection of GFP. Animals were anesthetized with ketamine:xylazine and perfused with 1× PBS followed by 4% (v/v) paraformaldehyde in 0.1M PBS. Brains were removed and postfixed for 24 hours in paraformaldehyde, followed by sucrose (30%) dehydration and embedded in OCT compound blocks. Anatomically matched free-floating coronal sections (35 μm thickness) from the rostral-to-caudal extent of the hypothalamus were collected and stored in 1× PBS with 0.02% sodium azide at 4°C. Free-floating sections were washed in PBS with 0.1% Triton (PBS-T) at room temperature 5 times for 10 minutes each time and then incubated overnight at 4°C with chicken anti-GFP antibody (1:5,000; GFP1020; Aves Labs), followed by incubation in donkey anti-chicken Alexa Fluor 488 (1:1,000; 703-545-155; Jackson ImmunoResearch). To provide a nuclear contrast stain, sections were incubated with DAPI (1:1000; MBD0015; Sigma-Aldrich) in PBS for 10 minutes at room temperature, followed by 3 washes in PBS-T and 2 additional washes in PBS. Sections were then mounted with polyvinyl acetate.

RT-PCR. Individual liver tissue samples were homogenized and RNA was isolated using Qiagen RNeasy Micro Kit (Kit 57805496, Hilden) and isolated RNA concentrations were quantified by Nanodrop (Thermo Fisher Scientific). Levels of specific transcripts were quantified by real-time PCR (ABI Prism 7900 HT; Applied Biosystems) using SYBR Green (Applied Biosystems) and the following specific primers: *Gck* (forward-CAAGCTGCACCCGAGCTT; reverse-TGATTCGATGAAGGTGATTTCG), *Pck1* (forward-GGCGGAGCATATGCTGATCC; reverse-CCACAGGCACTAGGGAAGGC), *G6pc* (forward-TCAACCTCGTCTTCAAGTGAGT; reverse-CTGCTTTATTATAGGCACGGAGCT). Expression levels of each gene were normalized to a house keeping gene (18S RNA) and standard curve. Nontemplate controls were incorporated into each PCR run.

Statistics

Results are expressed as Mean ± SEM. Significance was established at $P < 0.05$, 2-tailed. Serial measures of blood glucose, body weight, food intake, and ipGTT data between the 2 study groups were compared using a group-by-time mixed factorial repeated measures ANOVA with the Geisser-Greenhouse correction (GraphPad Software). For inter-

group comparisons, a 2-sample unpaired, 2-tailed Student's *t* test was applied. The collected data satisfied the normality assumptions necessary for the statistical analyses performed.

Study approval

All procedures were performed in accordance with the National Institutes of Health Guide for the Care and Use of Laboratory Animals and were approved by the Institutional Animal Care and Use Committee at the University of Washington, Seattle, WA.

Data availability

Values for all data points in graphs are reported in the Supporting Data Values file (<https://doi.org/10.1172/JCI189842DS1>). This file includes all raw data for each figure presented in the study. Additional datasets generated during and/or analyzed in the current study are not publicly available but are available from the corresponding author upon request.

Author contributions

YG, MG, JMS, GJM, and MWS designed the experiments. YG, MG, VD, CLF, CLB, BAP, AT, MKH, and JMS collected the data. YG, MG, VD, CLB, JMS, and GJM analyzed the data. YG, JMS, GJM, and MWS wrote the manuscript. All authors reviewed and edited the manuscript. MWS is the guarantor of this work and, thus, had full access to all the data in the study and takes responsibility for the accuracy and integrity of the data.

Acknowledgments

The authors gratefully acknowledge Jennifer Deem and Jenny Brown for their contributions to developing the experimental methodologies. In addition, the authors thank Kim Alonge and Zaman Mirzadeh for consulting on this study, Asmit Kumar for assistance with metabolic measurements, and Emily Quah and Kelly Kadlec for support with immunohistochemistry studies.

This work was supported by National Institutes of Health Grants DK083042 and DK101997 (to MWS), DK089056, DK124238, and S10OD036208 (to GJM), DK114474, DK128383, DoD W81XWH2110635 and P30 DK089507 (to JMS), the NIH-NIDDK funded Nutrition Obesity Research Center (NORC; P30DK035816), Diabetes Research Center (DRC; P30DK017047), and the Diabetes, Obesity and Metabolism Training Grant (T32 DK007247; CLF) at the University of Washington, a Department of Defense grant W81XWH2110635 (to JMS), a research agreement between MWS and Novo Nordisk, and a Cystic Fibrosis Foundation SINGH19R0 and SINGH24R0 (to YG).

Address correspondence to: Michael W. Schwartz, University of Washington Medicine Diabetes Institute, Department of Medicine, 750 Republican St Box 358055, Seattle, Washington 98195, USA. Phone: 1.206.897.5288; Email: mschwartz@u.washington.edu.

1. Brown JM, et al. Rethinking the role of the brain in glucose homeostasis and diabetes pathogenesis. *J Clin Invest.* 2019;129(8):3035–3037.
2. Mirzadeh Z, et al. Central nervous system control of glucose homeostasis: a therapeutic target for type 2 diabetes? *Annu Rev Pharmacol Toxicol.*

2022;62:55–84.

3. Mirzadeh Z, Faber C. Brain defense of glycemia in health and diabetes. *Diabetes.* 2024;73(12):1952–1966.
4. Scarlett JM, et al. Central injection of fibroblast growth factor 1 induces sustained remission

of diabetic hyperglycemia in rodents. *Nat Med.* 2016;22(7):800–806.

5. Bentsen MA, et al. Transcriptomic analysis links diverse hypothalamic cell types to fibroblast growth factor 1-induced sustained diabetes remission. *Nat Commun.* 2020;11(1):4458.

6. Wilson BD, et al. The role of agouti-related protein in regulating body weight. *Mol Med Today*. 1999;5(6):250–256.
7. Han Y, et al. Identification of a GABAergic neural circuit governing leptin signaling deficiency-induced obesity. *Elife*. 2023;12:e82649.
8. Hwang E, et al. Sustained inhibition of NPY/AgRP neuronal activity by FGF1. *JCI Insight*. 2022;7(17):e160891.
9. Scarlett JM, et al. Peripheral mechanisms mediating the sustained antidiabetic action of FGF1 in the brain. *Diabetes*. 2019;68(3):654–664.
10. Yki-Järvinen H. Fat in the liver and insulin resistance. *Ann Med*. 2005;37(5):347–356.
11. Dubuc PU, et al. Immunoreactive glucagon levels in obese-hyperglycemic (ob/ob) mice. *Diabetes*. 1977;26(9):841–846.
12. Edwardson JA, Hough CA. The pituitary-adrenal system of the genetically obese (ob/ob) mouse. *J Endocrinol*. 1975;65(1):99–107.
13. McGinnis R, et al. Dysregulation of the hypothalamus-pituitary-adrenal axis in male and female, genetically obese (ob/ob) mice. *J Neuroendocrinol*. 1992;4(6):765–771.
14. Solomon J, Mayer J. The effect of adrenalectomy on the development of the obese-hyperglycemic syndrome in ob-ob mice. *Endocrinology*. 1973;93(2):510–512.
15. German JP, et al. Leptin deficiency causes insulin resistance induced by uncontrolled diabetes. *Diabetes*. 2010;59(7):1626–1634.
16. Meek TH, et al. Evidence that in uncontrolled diabetes, hyperglucagonemia is required for ketosis but not for increased hepatic glucose production or hyperglycemia. *Diabetes*. 2015;64(7):2376–2387.
17. Fan S, et al. A neural basis for brain leptin action on reducing type 1 diabetic hyperglycemia. *Nat Commun*. 2021;12(1):2662.
18. Gonçalves GH, et al. Hypothalamic agouti-related peptide neurons and the central melanocortin system are crucial mediators of leptin's antidiabetic actions. *Cell Rep*. 2014;7(4):1093–1103.
19. Xu J, et al. Genetic identification of leptin neural circuits in energy and glucose homeostases. *Nature*. 2018;556(7702):505–509.
20. Brown JM, et al. The hypothalamic arcuate nucleus-median eminence is a target for sustained diabetes remission induced by fibroblast growth factor 1. *Diabetes*. 2019;68(5):1054–1061.
21. Douglass AM, et al. Neural basis for fasting activation of the hypothalamic-pituitary-adrenal axis. *Nature*. 2023;620(7972):154–162.
22. Orth DN. Cushing's syndrome. *N Engl J Med*. 1995;332(12):791–803.
23. Roberts BL, et al. Fibroblast growth factor-1 activates neurons in the arcuate nucleus and dorsal vagal complex. *Front Endocrinol (Lausanne)*. 2021;12:772909.
24. Loten EG, et al. In vivo studies on lipogenesis in obese hyperglycaemic (ob-ob) mice: possible role of hyperinsulinaemia. *Diabetologia*. 1974;10(1):45–52.
25. Schwartz MW, et al. Specificity of leptin action on elevated blood glucose levels and hypothalamic neuropeptide Y gene expression in ob/ob mice. *Diabetes*. 1996;45(4):531–535.
26. Schwartz MW, et al. Central nervous system control of food intake. *Nature*. 2000;404(6778):661–671.
27. Ebihara K, et al. Involvement of agouti-related protein, an endogenous antagonist of hypothalamic melanocortin receptor, in leptin action. *Diabetes*. 1999;48(10):2028–2033.
28. Mizuno TM, et al. Hypothalamic pro-opiomelanocortin mRNA is reduced by fasting and [corrected] in ob/ob and db/db mice, but is stimulated by leptin. *Diabetes*. 1998;47(2):294–297.
29. Mizuno TM, Mobbs CV. Hypothalamic agouti-related protein messenger ribonucleic acid is inhibited by leptin and stimulated by fasting. *Endocrinology*. 1999;140(2):814–817.
30. Andermann ML, Lowell BB. Toward a wiring diagram understanding of appetite control. *Neuron*. 2017;95(4):757–778.
31. Schwartz MW, et al. Leptin increases hypothalamic pro-opiomelanocortin mRNA expression in the rostral arcuate nucleus. *Diabetes*. 1997;46(12):2119–2123.
32. Thornton JE, et al. Regulation of hypothalamic proopiomelanocortin mRNA by leptin in ob/ob mice. *Endocrinology*. 1997;138(11):5063–5066.
33. German JP, et al. Leptin activates a novel CNS mechanism for insulin-independent normalization of severe diabetic hyperglycemia. *Endocrinology*. 2011;152(2):394–404.
34. Meek TH, Morton GJ. The role of leptin in diabetes: metabolic effects. *Diabetologia*. 2016;59(5):928–932.
35. Ring LE, Zeltser LM. Disruption of hypothalamic leptin signaling in mice leads to early-onset obesity, but physiological adaptations in mature animals stabilize adiposity levels. *J Clin Invest*. 2010;120(8):2931–2941.
36. van de Wall E, et al. Collective and individual functions of leptin receptor modulated neurons controlling metabolism and ingestion. *Endocrinology*. 2008;149(4):1773–1785.
37. Garfield AS, et al. Dynamic GABAergic afferent modulation of AgRP neurons. *Nat Neurosci*. 2016;19(12):1628–1635.
38. Cai J, et al. AgRP neurons are not indispensable for body weight maintenance in adult mice. *Cell Rep*. 2023;42(7):112789.
39. Zhu C, et al. Profound and redundant functions of arcuate neurons in obesity development. *Nat Metab*. 2020;2(8):763–774.
40. Stanley BG, Leibowitz SF. Neuropeptide Y injected in the paraventricular hypothalamus: a powerful stimulant of feeding behavior. *Proc Natl Acad Sci U S A*. 1985;82(11):3940–3943.
41. Marks JL, Waite K. Intracerebroventricular neuropeptide Y acutely influences glucose metabolism and insulin sensitivity in the rat. *J Neuroendocrinol*. 1997;9(2):99–103.
42. Zarjevski N, et al. Intracerebroventricular administration of neuropeptide Y to normal rats has divergent effects on glucose utilization by adipose tissue and skeletal muscle. *Diabetes*. 1994;43(6):764–769.
43. Essner RA, et al. AgRP neurons can increase food intake during conditions of appetite suppression and inhibit anorexigenic parabrachial neurons. *J Neurosci*. 2017;37(36):8678–8687.
44. Mc Morrow HE, et al. Incretin hormones and pharmacomimetics rapidly inhibit AgRP neuron activity to suppress appetite [preprint]. <https://doi.org/10.1101/2024.03.18.585583>. Posted on bioRxiv March 20, 2024.
45. Tong Q, et al. Synaptic release of GABA by AgRP neurons is required for normal regulation of energy balance. *Nat Neurosci*. 2008;11(9):998–1000.
46. Deem JD, et al. Cold-induced hyperphagia requires AgRP neuron activation in mice. *Elife*. 2020;9:e58764.
47. Faber CL, et al. Leptin receptor neurons in the dorsomedial hypothalamus regulate diurnal patterns of feeding, locomotion, and metabolism. *Elife*. 2021;10:e63671.
48. Taicher GZ, et al. Quantitative magnetic resonance (QMR) method for bone and whole-body-composition analysis. *Anal Bioanal Chem*. 2003;377(6):990–1002.
49. Kaiyala KJ, et al. Leptin signaling is required for adaptive changes in food intake, but not energy expenditure, in response to different thermal conditions. *PLoS One*. 2015;10(3):e0119391.
50. Weir JB. New methods for calculating metabolic rate with special reference to protein metabolism. *J Physiol*. 1949;109(1–2):1–9.
51. Burcelin R, et al. Acute intravenous leptin infusion increases glucose turnover but not skeletal muscle glucose uptake in ob/ob mice. *Diabetes*. 1999;48(6):1264–1269.
52. Halaas JL, et al. Physiological response to long-term peripheral and central leptin infusion in lean and obese mice. *Proc Natl Acad Sci U S A*. 1997;94(16):8878–8883.
53. Harris RB, et al. A leptin dose-response study in obese (ob/ob) and lean (+/?) mice. *Endocrinology*. 1998;139(1):8–19.
54. Kamohara S, et al. Acute stimulation of glucose metabolism in mice by leptin treatment. *Nature*. 1997;389(6649):374–377.
55. Li X, et al. Intracerebroventricular leptin infusion improves glucose homeostasis in lean type 2 diabetic MKR mice via hepatic vagal and non-vagal mechanisms. *PLoS One*. 2011;6(2):e17058.
56. Mistry AM, et al. Leptin rapidly lowers food intake and elevates metabolic rates in lean and ob/ob mice. *J Nutr*. 1997;127(10):2065–2072.
57. Morton GJ, Schwartz MW. Leptin and the central nervous system control of glucose metabolism. *Physiol Rev*. 2011;91(2):389–411.
58. Pellemounter MA, et al. Effects of the obese gene product on body weight regulation in ob/ob mice. *Science*. 1995;269(5223):540–543.